Surface Science 641 (2015) 278–281

Contents lists available at ScienceDirect

Surface Science

journal homepage: www.elsevier.com/locate/susc

Single PTCDA molecules on planar and stepped KCl and NaCl(100) surfaces

H. Aldahhak *, W.G. Schmidt, E. Rauls

Lehrstuhl für Theoretische Physik, Universität Paderborn, 33100 Paderborn, Germany

ARTICLE INFO

Available online 28 January 2015

Keywords:
DFT
PTCDA
KCl
NaCl
Step edges
PES

ABSTRACT

First principles calculations have been employed to investigate the adsorption of single PTCDA molecules on KCl(100) and NaCl(100) surfaces. The lateral and rotational diffusion barriers as well as the electronic and the geometric aspects of single PTCDA molecules adsorbed on planar terraces as well as at defective steps have been studied in detail.

1. Introduction

A great interest has been recently devoted to the adsorption of perylene-3,4,9,10-tetracarboxylic dianhydride (PTCDA) molecules ($C_{24}H_8O_6$) on different metallic and isolated surfaces [1–4]. This molecule shows a remarkable ability of forming well-defined long-range ordered arrangements as well as good epitaxial growth properties on various surfaces [5]. These properties can be ascribed to the non-uniform internal charge distribution within the molecular structure [6], shown schematically in Fig. 1.

On ionic surfaces, like KCl and NaCl, the adsorption of PTCDA molecules is mainly dominated by van-der-Waals and electrostatic forces [7,8], which arise between the partially charged atomic sites of the molecules and the ions of the surface [9–11]. Recent studies have shown that PTCDA molecules form commensurable long-range ordered monolayers on these surfaces [12,13].

Here, first principles calculations on the adsorption of single PTCDA molecules on both KCl(100) and NaCl(100) surfaces are presented. The paper is organized as follows: after introducing the methodology, we compare the adsorption of single PTCDA molecules on planar KCl(100) and NaCl(100) surfaces. Then, the translational as well as the rotational diffusion mechanisms of the molecule are studied. Finally, we discuss the adsorption of the molecules at step edges, which are energetically favorable.

Total-energy density functional calculations have been performed using the Vienna Ab Initio Simulation Package (VASP) [14]. Within the generalized gradient approximation (GGA), the formulation of the PW91 [15] has been used to model the electron exchange and correlation interactions. The projector-augmented wave (PAW) [16] method has been used to described the electron–ion interaction. The electronic wave functions are expanded into plane waves up to a kinetic energy of 400 eV. A semi-empirical scheme based on the London dispersion formula was used to approximately account for the influence of dispersion interactions [17]. Total-energy DFT calculations with this correction (DFT-D) yielded reliable results for various molecular adsorption systems (cf. Refs. [18–22]). Using the DFT-D approximation, our calculations predict the bulk lattice constants of KCl and NaCl within an error bar less than 1%. The integration of the Brillouin zone was done using a Γ-centered $2 \times 2 \times 1$ k-point mesh with a convergence criterion of 10^{-5} eV for the total energy. Six layer slabs were used to model the substrate in the supercell model. During structure optimization, the lowest two atomic layers were fixed to bulk positions, whereas, if not stated otherwise, the adsorbate and the four uppermost surface layers were allowed to relax freely until the forces were lower than 0.03 eV/Å. A vacuum layer of 40 Å separate the material slabs. Supercells of dimensions (4×4) surface unit cells have been used to model the single molecule adsorption in order to suppress unwanted interactions between periodic images of the molecule. The same setup was used to model the step edges in a saw tooth-like model system, described in [21]. Adsorption energies (E_{ads}) are calculated as:

$$E_{ads} = E_{sys} - E_{sur} - E_{mol},$$

where E_{sys} is the energy of the adsystem, E_{sur} and E_{mol} are the energies of the clean surface and the energy of the molecule in gas phase, respectively.

* Corresponding author at: Lehrstuhl für Theoretische Physik, Universität Paderborn, 33100 Paderborn, Germany.

http://dx.doi.org/10.1016/j.susc.2015.01.013
0039-6028/

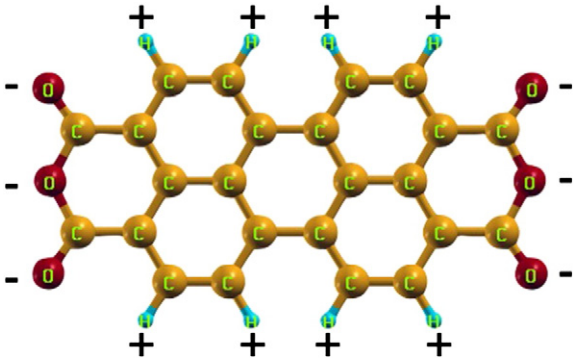

Fig. 1. Ball-and-stick model of the PTCDA molecule with partial charges distributed on its edges.

Table 1
Comparison between the different adsorption geometries of a single PTCDA molecule on KCl(100) and NaCl(100). With d_o, we express the distance between the carboxyl oxygen atoms of PTCDA and the surface ions beneath, while d_c expresses the distance between the center of the molecule and the surface ion beneath. The molecular anhydride-O-center-anhydride-O angle is denoted as θ. It expresses the downwards (upwards) molecular distortion angle in SQ_1 and R_1 (SQ_2 and R_2).

Structure	E_{ads} [eV]		d_o [Å]		d_c [Å]		θ	
	KCl	NaCl	KCl	NaCl	KCl	NaCl	KCl	NaCl
SQ_1	−2.49	−2.91	2.76	2.60	3.40	3.40	176.20	172
SQ_2	−1.62	−2.20	3.76	3.55	3.67	3.63	177.50	178.66
R_1	−2.13	−2.58	2.82	2.58	3.49	3.45	177.68	173.72
R_2	−1.85	−2.38	3.53	3.48	3.56	3.52	178.75	179.50

2. PTCDA on planar surfaces

For single PTCDA molecules on planar KCl and NaCl surfaces, various adsorption geometries have been tested and named as SQ_1, SQ_2, R_1 and R_2 (Fig. 2). In the SQ_1 and SQ_2 (R_1 and R_2) structures, the molecular long-axis is parallel to the [110] ([100]) direction of the surface. The center of the molecule is on top of an anion site in SQ_1 and R_1, while it is above a cation site in SQ_2 and R_2. The carboxyl oxygen atoms of the molecule are above two cation atoms of the surface in SQ_1 and R_1, while they are above two anion sites of the surface in SQ_2 and R_2. In agreement with previous experimental and theoretical works [22,21,23], the so-called SQ_1 is the most favorable structure on both KCl(100) and Na(100) surfaces. Compared to KCl(100), single PTCDA molecules show higher adsorption energies and stronger distortion on NaCl(100) (cf. Table 1). This has previously been ascribed to the better lattice match between the carboxyl oxygen atoms of the molecule and the cations of the NaCl surface [21].

After having determined the most favorable structures of single molecules on both surfaces, we compared their lateral diffusion barriers by calculating the corresponding potential energy surfaces (PESs) (Fig. 3 *left*). Taking the molecular center as a reference and keeping the molecular long-axis parallel to the [110] direction of the surface, the molecular adsorption energies are sampled on a dense lateral grid of points separated by 0.1 Å throughout the surface unit cell (Fig. 3 *left*). In order to assure the position of the reference, the two carbons (indicated green in Fig. 3 *left*) are fixed laterally, while all other atoms are allowed to move and relax freely. On KCl (NaCl), our calculations show a maximum corrugation of 0.87 eV (0.71 eV) for the PES and diffusion barriers of 0.58 eV (0.48 eV) as well as a low energy anion–anion diffusion channel (Fig. 3 *left*). Single PTCDA molecules avoid structures where their centers are above the surface cations (SQ_2). The lateral diffusion barriers on NaCl are smaller than on KCl. This might be due to the smaller lattice constant in case of NaCl. In a recent study of PTCDA on KCl(100) [22], it has been found that the compression of the KCl lattice constant by 5% decreases the lateral diffusion barriers by 0.1 eV. It should be noted that the full relaxation of both the lateral degrees of freedom and the orientation of the molecules can be expected to lower the diffusion barriers.

Fig. 3, center and hand right side, shows the adsorption energy as a function of the molecular rotation angle. Adsorption energies have been calculated for angles between $\theta = 0^o$ and $\theta = 90^o$, which correspond to the [100] and [010] directions of the surface. The energy of the molecule in SQ_1 is considered as zero on the energy scale ($\theta = 45^o$ in Fig. 3). On both KCl and NaCl, we found that PTCDA shows rotation barriers of 0.53 eV. The maximum is reached for an angle of ($\theta = 18^o$ and $\theta = 72^o$) for both surfaces. According to the lateral and rotational barriers, we confirm SQ_1 to be the global energy minimum on both surfaces, while the adsorption configuration with the molecular axis parallel to [100] (R_1) represents a local energy minimum. This most favorable 45^o orientation can be reached by an activation energy of less than 0.15 eV (for KCl)/0.20 eV (for NaCl).

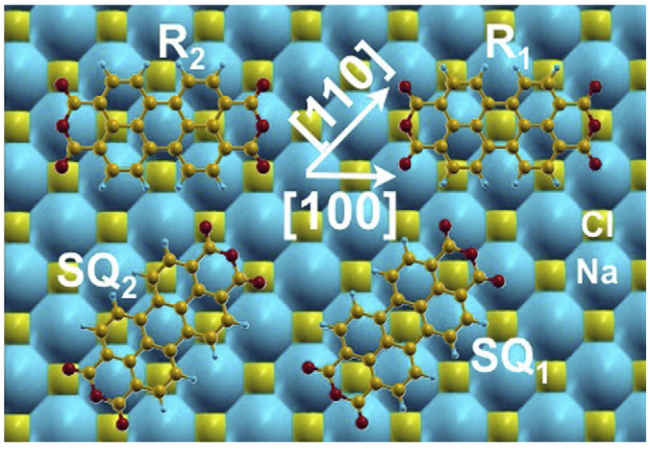

Fig. 2. Single PTCDA molecules adsorbed on a planar NaCl(100) surface. The different adsorption structures (see text) are shown.

3. Adsorption at step-edges

The adsorption of PTCDA molecules at NaCl and KCl step edges has been studied experimentally by Karacuban et al. [6] and Guo et al. [22]. Defective step edges oriented along <100> have been proven to be preferred adsorption sites for single PTCDA molecules on both KCl and NaCl surfaces. This result agrees with fluorescence spectroscopy experiments [23] and DFT calculations (cf. Ref. h-aldahhak-2013 and guo2014). At both KCl and NaCl steps, the so-called vacancy site has been identified to be the most favorable defective site [6,21,22]. Here, the PTCDA molecule is embedded into the step-edge with its long axis in the same orientation as on the planar surface [21–23].

We modeled the different possible defect sites and calculated the molecular adsorption energies (lower panel of Fig. 4). These sites are: the non-polar (T), the non-polar (S), the Cl-terminated and the K/Na-terminated step edges, various inequivalent kink sites (K/Na-terminated or Cl-terminated), and the vacancy sites (Fig. 4). Irrespective of the defect type, the registry of the molecule is similar to that on the planar surface. Its long axis is parallel to <110> except for the non-polar (S) site. In this case, the molecular long axis is parallel to [010] and the registry of the molecule is similar to R_1. The adsorption energies of PTCDA on these sites are given in Table 2.

In agreement with the experimental results [23,22], step edges are thermodynamically favored over terraces sites. For both KCl and NaCl,

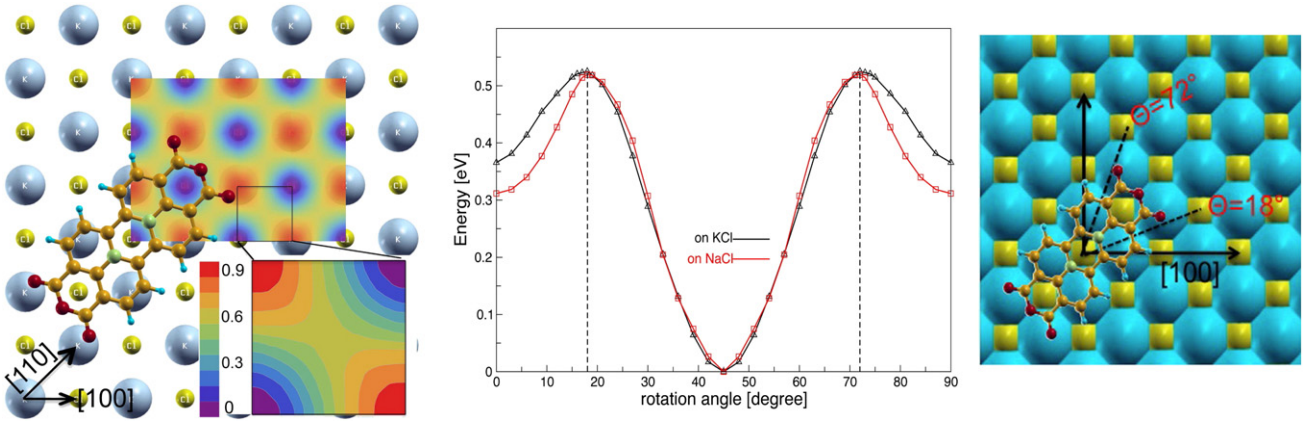

Fig. 3. (*left*) Calculated potential energy surface (PES) for PTCDA on KCl(100). The energy of the most favored structure (SQ_1) corresponds to zero energy (in eV). The less favorable adsorption configurations have, then, positive energies. The indicated green inner atoms were laterally fixed (see text for details). For NaCl, a similar map is calculated (not shown) with different corrugation of the surface 0.71 eV (0.87 eV for KCl) and diffusion barriers of 0.48 eV (0.58 eV for KCl). (middle) The calculated rotational energy barriers of single PTCDA molecules on KCl(001) and NaCl(100). The molecular long axis forms an angle (θ) with respect to the substrate [100] direction (*right*). The energy of the molecule in the energetically most favored structure (SQ_1) is chosen as zero energy. It forms an angle of $\theta = 45^{o}$.

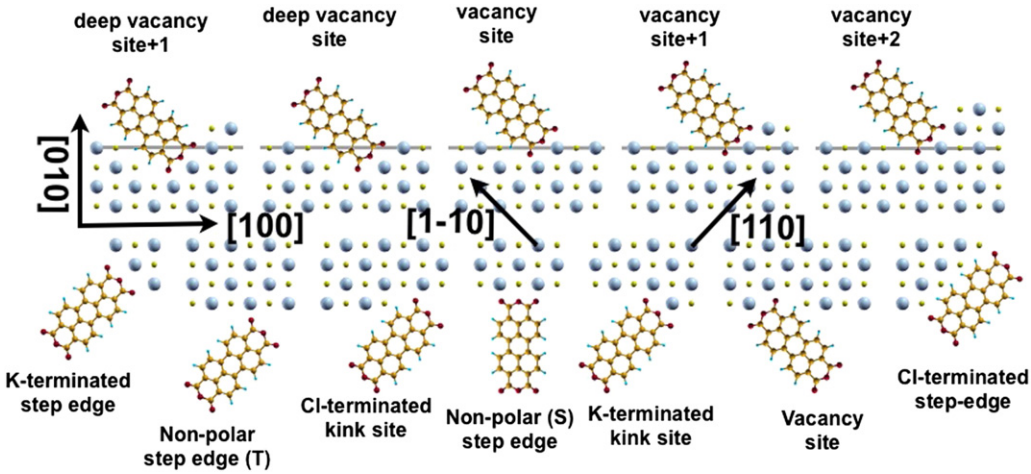

Fig. 4. Different suggested models of defect-free and defected KCl step-edges are shown in the lower part. The orientations of PTCDA molecules with respect to the surface and to the step-edge orientations are shown. In the upper part, the different suggested models of vacancies are shown. A depicted gray line shows the further molecular embedding into the step-edges in the deep-vacancy (deep-vacancy + 1) site compared to a simple vacancy site.

the vacancy site is the most probable site between the different suggested defective sites (Table 2). The molecular orientation fits with the experimental expectation for KCl [23]. Compared to the terraces sites, the energy gain is 0.79 eV and 1.22 eV on KCl and NaCl, respectively, i.e., of the same order of magnitude as the activation energies.

Starting from the adsorption at a vacancy site, even more favorable adsorption sites may be obtained by deepening the vacancy. This is, e.g., realized by adding an extra row or several rows of KCl to the step edges close to the vacancy. These configurations take advantage of the PTCDA charge distribution (cf. Fig. 2). The corresponding models are shown in the upper panel of Fig. 4. Both symmetric and asymmetric vacancy models have been considered. Table 3 summarizes the adsorption energies for these structures. As could be expected based on the charge distribution of the molecule, the deep vacancy sites are the most stable ones due to the optimized interaction between the surface ions and the molecular partial charges.

On KBr, which is a similar surface to both KCl and NaCl with larger lattice constant (6.6 Å), PTCDA behaves similarly [24]. PTCDA molecules have on the planar KBr surfaces similar registries like those on KCl and NaCl. The defective KBr step-edges sites are, also, more favorable adsorption sites compared to those on the planar surface. However, because of the larger lattice constant of KBr, compared to KCl and NaCl, the adsorption energy amounts to −2.36 eV [24].

In summary, we compared the adsorption of single PTCDA molecules on two similar ionic surfaces with different lattice constants, i.e., KCl(100) and NaCl(100). Results are similar for the two surfaces, but we obtain in general higher adsorption energies and stronger

Table 2
Calculated adsorption energies (in eV) of PTCDA at flat terraces and at the adsorption sites illustrated in the lower panel of Fig. 4.

Site	KCl	NaCl
Terraces sites	−2.49	−2.91
Non-polar step edge (S)	−2.41	−3.05
Non-polar step edge (T)	−2.57	−3.31
K-terminated step edges	−3.05	−3.80
Cl-terminated step edges	−2.90	−3.47
K-terminated kink site	−2.86	−3.64
Cl-terminated Kink site	−2.70	−3.60
Vacancy site	−3.28	−4.13

Table 3
Calculated adsorption energies of PTCDA energies for different types of vacancy sites at KCl step edges illustrated in the upper panel of Fig. 4.

Model of vacancy site	adsorption energy (eV)
Vacancy site	−3.28
Vacancy site + 1	−3.44
Vacancy site + 2	−3.47
Deep vacancy site	−3.75
Deep vacancy site + 1	−3.76

distortion for NaCl. The same holds for the diffusion barriers and for the adsorption of the molecule at step edges. The smaller lattice constant for NaCl results in lower lateral diffusion barriers for PTCDA molecules on NaCl compared to KCl.

Calculations were performed on the Paderborn Center for Parallel Computing (PC2). For the financial support, the authors acknowledge the Deutsche Forschungsgesellschaft (D-A-CH project FWF I958 and GRK 1464).

References

[1] M. Mura, X. Sun, F. Silly, H.T. Jonkman, G.A.D. Briggs, M.R. Castell, L.N. Kantorovich, Phys. Rev. B 81 (2010) 195412.
[2] O. Bauer, G. Mercurio, M. Willenbockel, W. Reckien, C. Heinrich Schmitz, B. Fiedler, S. Soubatch, T. Bredow, F.S. Tautz, M. Sokolowski, Phys. Rev. B 86 (2012) 235431.
[3] M. Müller, J. Ikonomov, M. Sokolowski, Surf. Sci. 605 (2011) 1090.
[4] M. Müller, E. Le Moal, R. Scholz, M. Sokolowski, Phys. Rev. B 83 (2011) 241203.
[5] A.L.R. Temirov, S. Soubatch, F.S. Tautz, Nature 444 (2006) 350.
[6] H. Karacuban, S. Koch, M. Fendrich, Th. Wagner, R. Möller, Nanotechnology 22 (2011) 295305.
[7] T. Trevethan, A.L. Shluger, J. Phys. Chem. C 111 (2007) 15375.
[8] B. Hoff, M. Gingras, R. Peresutti, C.R. Henry, A.S. Foster, C. Barth, J. Phys. Chem. C 118 (2014) 14569.
[9] P. Rahe, M. Kittelmann, J.L. Neff, M. Nimmrich, M. Reichling, P. Maass, A. Kühnle, Adv. Mater. 25 (2013) 3948.
[10] B. Such, T. Trevethan, T. Glatzel, S. Kawai, L. Zimmerli, E. Meyer, A.L. Shluger, C.H.M. Amijs, P. de Mendoza, A.M. Echavarren, ACS Nano 4 (2010) 3429.
[11] L. Nony, F. Bocquet, F. Para, F. Chérioux, E. Duverger, F. Palmino, V. Luzet, C. Loppacher, Beilstein J. Nanotechnol. 3 (2012) 285.
[12] T. Dienel, C. Loppacher, S.C.B. Mannsfeld, R. Forker, T. Fritz, Adv. Mater. 20 (2008) 959.
[13] E. Le Moal, M. Müller, O. Bauer, M. Sokolowski, Phys. Rev. B 82 (2010) 045301.
[14] G. Kresse, J. Furthmüller, Comput. Mater. Sci. 6 (1996) 15.
[15] J.P. Perdew, J.A. Chevary, S.H. Vosko, K.A. Jackson, M.R. Pederson, D.J. Singh, C. Fiolhais, Phys. Rev. B 46 (1992) 6671.
[16] G. Kresse, D. Joubert, Phys. Rev. B 59 (1999) 1758.
[17] F. Ortmann, F. Bechstedt, W.G. Schmidt, Phys. Rev. B 73 (2006) 205101.
[18] E.R. McNellis, J. Meyer, K. Reuter, Phys. Rev. B 80 (2009) 205414.
[19] C. Thierfelder, M. Witte, S. Blankenburg, E. Rauls, W.G. Schmidt, Surf. Sci. 605 (2011) 746.
[20] E. Rauls, T. Pertram, W.G. Schmidt, K. Wandelt, Surf. Sci. 606 (2012) 1120.
[21] H. Aldahhak, W.G. Schmidt, E. Rauls, Surf. Sci. 617 (2013) 242.
[22] Q. Guo, A. Paulheim, M. Sokolowski, H. Aldahhak, E. Rauls, W.G. Schmidt, J. Phys. Chem. C 118 (2014) 29911.
[23] A. Paulheim, M. Müller, C. Marquardt, M. Sokolowski, Phys. Chem. Chem. Phys. 15 (2013) 4906.
[24] O.H. Pakarinen, J.M. Mativetsky, A. Gulans, M.J. Puska, A.S. Foster, P. Grutter, Phys. Rev. B 80 (2009) 085401.